Complexity in pulsed nonlinear laser systems interrogated by permutation entropy

Joshua P. Toomey,[1,*] Deborah M. Kane,[1] and Thorsten Ackemann[2]

[1]*MQ Photonics Research Centre, Dept. of Physics & Astronomy, Macquarie University, Sydney, 2109, Australia*
[2]*SUPA and Dept. of Physics, University of Strathclyde, Glasgow G4 0NG, UK*
[*]*josh.toomey@mq.edu.au*

Abstract: Permutation entropy (PE) has a growing significance as a relative measure of complexity in nonlinear systems. It has been applied successfully to measuring complexity in nonlinear laser systems. Here, PE and weighted permutation entropy (WPE) are discovered to show an unexpected inversion to higher values, when characterizing the complexity at the characteristic frequencies of nonlinear drivers in laser systems, for output power sequences which are pulsed. The cause of this inversion is explained and its presence can be used to identify when irregular dynamics transform into a fairly regular pulsed signal (with amplitude and timing jitter). When WPE is calculated from experimental output power time series from various nonlinear laser systems as a function of delay time, both the minimum value of WPE, and the width of the peak in the WPE plot are shown to be indicative of the level of amplitude variation and timing jitter present in the pulsed output. Links are made with analysis using simulated time series data with systematic variation in timing jitter and/or amplitude variations.

OCIS codes: (140.1540) Chaos; (140.3538) Lasers, pulsed; (140.3580) Lasers, solid-state; (140.5960) Semiconductor lasers; (140.7260) Vertical cavity surface emitting lasers.

References and links

1. P. Grassberger and I. Procaccia, "Measuring the strangeness of strange attractors," Physica D **9**(1-2), 189–208 (1983).
2. M. T. Rosenstein, J. J. Collins, and C. J. Deluca, "A practical method for calculating largest Lyapunov exponents from small data sets," Physica D **65**(1-2), 117–134 (1993).
3. H. Kantz, "A robust method to estimate the maximal Lyapunov exponent of a time-series," Phys. Lett. A **185**(1), 77–87 (1994).
4. H. Kantz and T. Schreiber, Nonlinear Time Series Analysis, 2nd ed. (Cambridge University Press, Cambridge, 2004).
5. C. Bandt and B. Pompe, "Permutation entropy: A natural complexity measure for time series," Phys. Rev. Lett. **88**(17), 174102 (2002).
6. M. T. Martin, A. Plastino, and O. A. Rosso, "Generalized statistical complexity measures: Geometrical and analytical properties," Physica A **369**(2), 439–462 (2006).
7. Y. H. Cao, W. W. Tung, J. B. Gao, V. A. Protopopescu, and L. M. Hively, "Detecting dynamical changes in time series using the permutation entropy," Phys. Rev. E Stat. Nonlin. Soft Matter Phys. **70**(4), 046217 (2004).
8. L. Zunino, O. A. Rosso, and M. C. Soriano, "Characterizing the hyperchaotic dynamics of a semiconductor laser subject to optical feedback via permutation entropy," IEEE J. Sel. Top. Quantum Electron. **17**(5), 1250–1257 (2011).
9. M. C. Soriano, L. Zunino, O. A. Rosso, I. Fischer, and C. R. Mirasso, "Time scales of a chaotic semiconductor laser with optical feedback under the lens of a permutation information analysis," IEEE J. Quantum Electron. **47**(2), 252–261 (2011).
10. J. P. Toomey and D. M. Kane, "Mapping the dynamic complexity of a semiconductor laser with optical feedback using permutation entropy," Opt. Express **22**(2), 1713–1725 (2014).
11. J. Tiana-Alsina, M. C. Torrent, O. A. Rosso, C. Masoller, and J. Garcia-Ojalvo, "Quantifying the statistical complexity of low-frequency fluctuations in semiconductor lasers with optical feedback," Phys. Rev. A **82**(1), 013819 (2010).

#208715 - $15.00 USD Received 24 Mar 2014; revised 5 May 2014; accepted 4 Jul 2014; published 16 Jul 2014

12. N. Rubido, J. Tiana-Alsina, M. C. Torrent, J. Garcia-Ojalvo, and C. Masoller, "Language organization and temporal correlations in the spiking activity of an excitable laser: Experiments and model comparison," Phys. Rev. E Stat. Nonlin. Soft Matter Phys. **84**(2), 026202 (2011).
13. A. Aragoneses, N. Rubido, J. Tiana-Alsina, M. C. Torrent, and C. Masoller, "Distinguishing signatures of determinism and stochasticity in spiking complex systems," Sci. Rep. **3**, 1778 (2013).
14. S. Valling, T. Fordell, and A. M. Lindberg, "Maps of the dynamics of an optically injected solid-state laser," Phys. Rev. A **72**(3), 033810 (2005).
15. Y. Tanguy, T. Ackemann, W. J. Firth, and R. Jäger, "Realization of a Semiconductor-Based Cavity Soliton Laser," Phys. Rev. Lett. **100**(1), 013907 (2008).
16. N. Radwell and T. Ackemann, "Characteristics of Laser Cavity Solitons in a Vertical-Cavity Surface-Emitting Laser With Feedback From a Volume Bragg Grating," IEEE J. Quantum Electron. **45**(11), 1388–1395 (2009).
17. D. M. Kane and J. P. Toomey, "Variable pulse repetition frequency output from an optically injected solid state laser," Opt. Express **19**(5), 4692–4702 (2011).
18. J. P. Toomey, D. M. Kane, S. Valling, and A. M. Lindberg, "Automated correlation dimension analysis of optically injected solid state lasers," Opt. Express **17**(9), 7592–7608 (2009).
19. T. Ackemann, N. Radwell, C. McIntyre, G. L. Oppo, and W. J. Firth, "Self pulsing solitons: A base for optically controllable pulse trains in photonic networks?" in Transparent Optical Networks (ICTON), 2010 12th International Conference on, 2010), 1–4.
20. N. Radwell, "Characteristics of a cavity soliton laser based on a VCSEL with frequency selective feedback," PhD Thesis (University of Strathclyde, 2010).
21. M. Staniek and K. Lehnertz, "Parameter selection for permutation entropy measurements," Int. J. Bifurcat. Chaos **17**(10), 3729–3733 (2007).
22. B. Fadlallah, B. Chen, A. Keil, and J. Príncipe, "Weighted-permutation entropy: A complexity measure for time series incorporating amplitude information," Phys. Rev. E Stat. Nonlin. Soft Matter Phys. **87**(2), 022911 (2013).
23. J. P. Toomey, D. M. Kane, M. W. Lee, and K. A. Shore, "Nonlinear dynamics of semiconductor lasers with feedback and modulation," Opt. Express **18**(16), 16955–16972 (2010).

1. Introduction

Characterization of complex signals can provide a number of useful insights into the nature of the nonlinear systems that produce them. There are a number of techniques used to characterize time series such as dimensional analysis [1], largest Lyapunov exponents [2, 3], various entropies [4, 5], and statistical complexity measures [6]. One of the most useful and easily implemented, and the one employed in this study, is the permutation entropy [5]. Permutation entropy (PE) is a conceptually simple idea for quantifying complexity based on ordinal patterns in time series data. The method of generating the probability distributions on which the entropy is calculated (explained in Section 2) means the result is a relative measure of time series predictability. Permutation entropy analysis is easily implemented and computationally much faster than other techniques such as Lyapunov exponents [7], while being robust to noise [8].

PE analysis has been applied to time series data of the output power fluctuations in a semiconductor laser with delayed optical feedback [8–10]. It was shown that chaotic time series show reduced complexity on time scales that correspond to key characteristic frequencies of the dynamic system (i.e. the external cavity round trip delay time and its harmonics and sub-harmonics). Similar techniques have been used to characterize the intervals between power dropouts in semiconductor laser with optical feedback operating in a low-frequency fluctuation regime [11–13]

Not all nonlinear laser systems produce dynamics which are as complex as the conventional optical feedback setup. In this work we consider two other experimental laser systems, an optically injected solid state laser (OISSL) [14] and a broad-area vertical cavity surface emitting laser (VCSEL) with frequency selective feedback [15, 16]. Both of these systems, when operated with appropriate parameter settings, produce less complex dynamics than that seen in a semiconductor laser with optical feedback (SLWOF) system. The OISSL system, subject to variation of injection strength and frequency detuning of the injected light, produces spiky, pulse-like output power that can have a continuously variable dominant repetition frequency [17] and chaotic variation in spike amplitude [18], depending on the system parameters. The VCSEL system displays a similar spiky output [19, 20], although not as clean as that seen in some regions of the OISSL operating parameter space. Application of

#208715 - $15.00 USD Received 24 Mar 2014; revised 5 May 2014; accepted 4 Jul 2014; published 16 Jul 2014

PE analysis to these pulsed output power time series shows the expected drop in entropy for time scales approaching the dominant frequencies, but, unexpectedly, the central part of this 'dip' is inverted and an increase in complexity (PE) at time scales matching the characteristic frequencies of each system is observed. This 'inverted-dip' peak is associated with the complexity in the amplitude and timing variations between power spikes and can be employed to indicate when a time series is nearly pulsed, in practice a signal that is spiking with varying amplitude and/or a slightly irregular period. It is also shown that the width of the PE peak at these frequencies can be linked to the amount of variation, in particular the timing jitter between pulses, but also the amplitude variation.

2. Permutation entropy

The degree of disorder or uncertainty in a system can be quantified by a measure of entropy. The uncertainty associated with a physical process described by the probability distribution $P=\{p_i, i=1,...,\mathrm{M}\}$ is related to the Shannon entropy,

$$S[P]=-\sum_{i=1}^{M} p_i \ln p_i \quad . \tag{1}$$

Constructing probability distributions using ordinal patterns from recorded time series was proposed by Bandt and Pompe [5]. The benefit of using this symbolic approach is improved robustness to noise and invariance to nonlinear monotonous transformations (e.g. measurement equipment drift) when compared with other complexity measures [5]. This is due to the way the ordinal patterns are constructed based on the relative amplitude of time series values and makes it particularly attractive for use on experimental data.

The Bandt and Pompe process of generating the probability distribution is described in detail elsewhere [5, 9]. It is briefly outlined here. To obtain the ordinal pattern distribution on which to calculate entropy, one must first choose an appropriate ordinal pattern length D and ordinal pattern delay τ. There are $D!$ possible permutations for a vector of length D, so in order to obtain reliable statistics the length of the time series N should be much larger than D [21].

The time scale over which the complexity is quantified can be set by changing the ordinal pattern delay τ. This is the time separation between values used to construct the vector from which the ordinal pattern is determined. Its value corresponds to a multiple of the signal sampling period. For a given time series $\{x_t, t=1,...,N\}$, ordinal pattern length D, and ordinal pattern delay τ, we consider the vector

$$X_S \rightarrow \left(x_{s-(D-1)\tau}, x_{s-(D-2)\tau}, ..., x_{s-\tau}, x_s\right) \quad . \tag{2}$$

At each time s the ordinal pattern of this vector can be converted to a unique symbol $\pi=(r_0, r_1, ..., r_{D-1})$ defined by

$$x_{s-r_0\tau} \geq x_{s-r_1\tau} \geq ... \geq x_{s-r_{D-2}\tau} \geq x_{s-r_{D-1}\tau} \quad . \tag{3}$$

The ordinal pattern probability distribution $P=\{p(\pi_i), i=1,...,D!\}$ required for the entropy calculation is constructed by determining the relative frequency of all the $D!$ possible permutations π_i. The normalized permutation entropy is then defined as the normalized Shannon entropy S associated with the permutation probability distribution P,

$$\mathcal{H}_S[P]=\frac{S[P]}{S_{\max}}=\frac{-\sum_{i=1}^{D!} p(\pi_i)\ln p(\pi_i)}{\ln D!} \tag{4}$$

#208715 - $15.00 USD Received 24 Mar 2014; revised 5 May 2014; accepted 4 Jul 2014; published 16 Jul 2014

This normalized permutation entropy gives values $0 \le \mathcal{H}_S \le 1$ where a completely predictable time series has a value of 0 and a completely stochastic process with a uniform probability distribution is represented by a value of 1. It is important to realize that the PE is a statistical measure and is not able to distinguish whether the observed complexity (irregularity) arises from stochastic or deterministic chaotic processes. It is also important that the PE provides means to characterize complexity on different time scales, given by the ordinal pattern delay.

As it was originally defined, the permutation entropy retains no information about the amplitude of the signal apart from the relative order structure. A recent publication describes a modification to the algorithm to generate a weighted permutation entropy which incorporates amplitude information from the signal, in addition to the ordinal patterns [22]. The procedure for calculating the weighted permutation entropy (WPE) is briefly described here.

Instead of each sub vector X_s, which matches a certain permutation, contributing equally to the entropy, each is weighted using the variance by,

$$w_s = \frac{1}{D}\sum_{k=1}^{D}\left[x_{s-(k-1)\tau} - \bar{X}_S \right]^2 \tag{5}$$

Where $\bar{X}_S$ is the arithmetic mean of the sub vector X_s defined in Eq. (2). This definition retains the general properties of the original PE algorithm whilst incorporating amplitude information and more robustness to noise. In this study we employ this weighted PE as it is more appropriate for analysis of pulse-like time series [22].

3. Experimental results

3.1 Results for conventional delayed optical feedback

Calculation of the permutation entropy as a function of ordinal pattern delay τ quantifies the relative complexity of the time series on different time scales. This analysis has been previously applied to output power time series from semiconductor lasers with optical feedback (SLWOF) operating in a chaotic region of its parameter space, and has identified time scales associated with key frequencies inherent to the system being studied [9]. The plot in Fig. 1 shows calculations of both the original PE and weighted PE as a function of ordinal pattern delay for an experimental time series (sampled at 50 ps) generated by the SLWOF system operated in a region of high injection (injection current = 68.7 mA) and high feedback (intra-cavity AOM transmission of 64.4%, see [10] for details). In this example the number of points in the time series in N = 20,000 and we use ordinal pattern length D = 5. This ensures $N \gg D!$ and keeps the computation time practical. The PE and WPE show dips indicating reduced complexity at time scales matching the external cavity (τ_{ext}) and relaxation oscillation (τ_{RO}) frequencies, and integer fractions of these [10]. Note that the WPE gives qualitatively the same results as the original PE algorithm, albeit with greater definition of the key features.

#208715 - $15.00 USD Received 24 Mar 2014; revised 5 May 2014; accepted 4 Jul 2014; published 16 Jul 2014

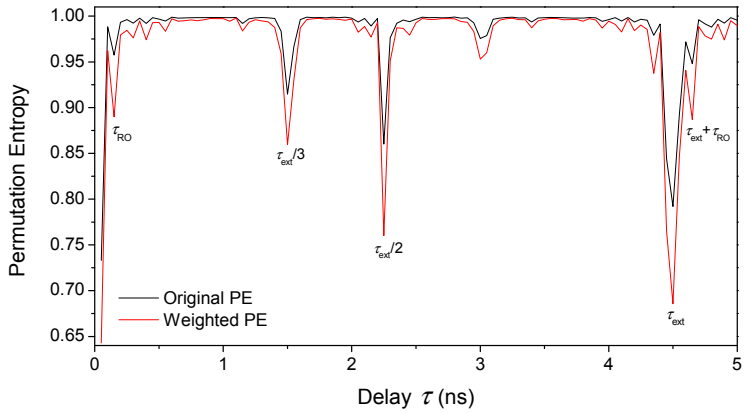

Fig. 1. Permutation entropy (black) and weighted PE (red) for $D = 5$ as a function of ordinal pattern delay τ for a time series record of optical power (20GSa/s sampling rate) from a semiconductor laser with optical feedback (injection current = 68.7 mA, intra-cavity AOM transmission = 0.644, cavity round trip time τ_{ext} = 4.5 ns and relaxation oscillation period = 150 ps) [10].

The interpretation of this data is that the dynamics is quite irregular in general for most time scales but becomes more regular and predictable at the laser cavity round-trip time (τ_{ext}), the period corresponding to the relaxation oscillation frequency (τ_{RO}) and multiples or fractions of these.

When applying this technique to data which is somewhat more regular, such as nearly periodic, pulsed time series, we see a central inverted peak occur within the dip in the value of permutation entropy for ordinal pattern delays τ that correspond to the pulse period. A number of examples of this type of behavior have been observed and analyzed. They are describe in more detail in the following sections.

3.2 Vertical-cavity surface-emitting laser with frequency-selective feedback

The first example is a vertical-cavity surface-emitting laser (VCSEL) with frequency-selective optical feedback [16]. A broad-area VCSEL (980 nm emission wavelength, 200 μm diameter) is coupled to a volume Bragg grating as narrow-band frequency filter via a self-imaging cavity. The round trip time in the external cavity is 0.61 ns. Close to threshold the system displays lasing on small, localized lasing spots within the broad-area aperture, which are interpreted as cavity solitons [16].

In narrow parameter regions, these solitons display self-pulsing [19, 20]. The example is shown in Fig. 2(a) is an output power time series consisting of 30,000 pts recorded from a 12 GHz detector on a 18 GHz oscilloscope with 60 GSa/s sampling rate. It is quite spiky with a dominant frequency of 3.3 GHz (i.e. the harmonic of the round-trip frequency) but with significant variation in spike amplitude. This time scale is picked up in the WPE analysis as peaks occurring for values of τ at multiples of ~0.3 ns, seen in Fig. 2(b). The peaks indicate a higher irregularity at the round-trip frequency and harmonics/sub-harmonics. Interestingly, the peaks are not sitting on a flat background but there are indications for an undershoot before and after the main peak, i.e. the peaks might be interpreted as a central narrow spike on a broader minimum. This observation will be supported by the discussion of the data in Sec. 3.3.

The same qualitative features are obtained for other nearly-periodic time series observed for nearby parameters and having a dominant spiking interval at the round-trip time.

#208715 - $15.00 USD Received 24 Mar 2014; revised 5 May 2014; accepted 4 Jul 2014; published 16 Jul 2014

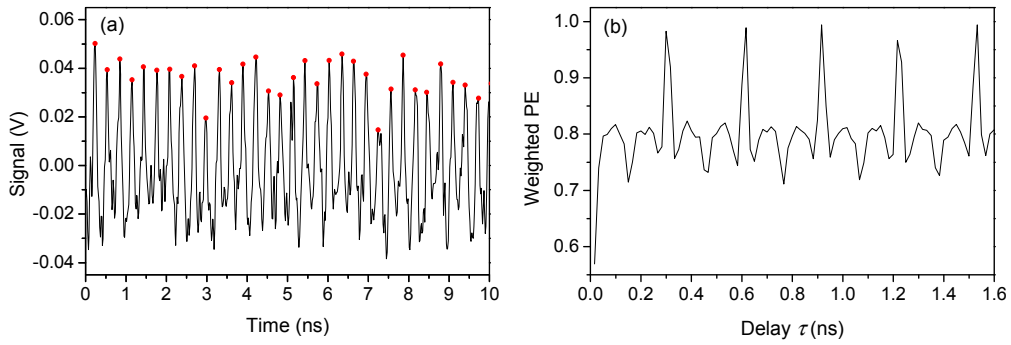

Fig. 2. (a) Time series record of optical power from a single soliton in a VCSEL with frequency selective optical feedback, and (b) weighted PE (D = 5) as a function of ordinal pattern delay τ. The data are taken with an AC-coupled 12 GHz detector, amplified with a 15 GHz RF amplifier and digitized with a 18 GHz oscilloscope at 60 Gs/s (16.7 ps sampling time, 30000 points).

3.3 Solid state laser with optical injection

Another example of pulsed dynamics is shown in Fig. 3 for an optically injected solid state laser (OISSL) [14, 17]. This data was recorded with the laser operating in a relatively stable region of the parameter space with normalized frequency detuning $\Delta\omega = -1.849$ and normalized injection strength $K = 0.226$. Both these experimentally measured quantities were normalized to the angular relaxation oscillation frequency (see [14] for details). The signal was sampled at 10 ns and each time series contained 5000 points. In this case, the time varying signal, seen in Fig. 3(a), is much more pulse-like, with less variation in pulse amplitude, and has a higher signal-to-noise ratio (SNR = 17.18), compared with the VCSEL system (SNR = 2.74). The pulse repetition frequency is 4 MHz. The resulting WPE plot, shown in Fig. 3(b), shows a narrow spike within a broader valley at values of τ equal to multiples of the pulse period. This matches the previous observation for the VCSEL of an increase in complexity at ordinal pattern delays corresponding to the pulse period, however there is a much more noticeable drop either side of the peak than was observed in the VCSEL plot in Fig. 2(b).

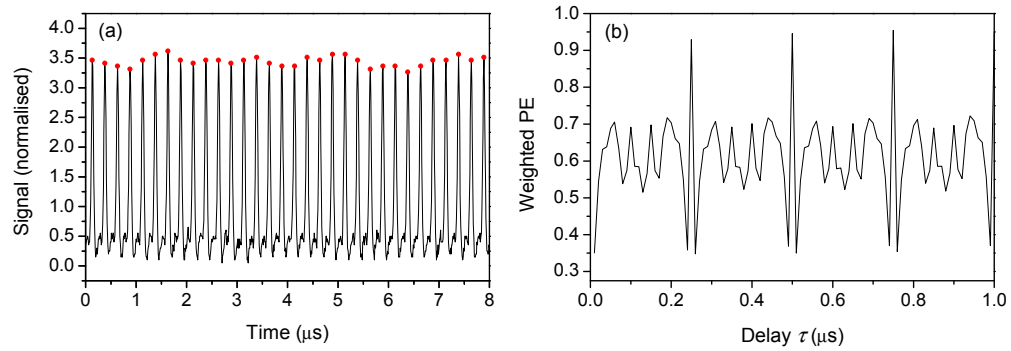

Fig. 3. (a) Output power time series from an optically injected solid state laser (normalized frequency detuning $\Delta\omega = -1.849$ and normalized injection strength $K = 0.226$) [14], and (b) weighted PE (D = 5) as a function of ordinal pattern delay. Signal was sampled at 10ns and trace contained 5000 data points (50 μs).

3.4 Discussion of experimental results

The reduction of complexity close to the characteristic pulsing frequency is due to the way PE/WPE characterizes complexity based on the order of points in the sub vector used to

#208715 - $15.00 USD Received 24 Mar 2014; revised 5 May 2014; accepted 4 Jul 2014; published 16 Jul 2014

assign a permutation symbol. As the ordinal pattern delay used in the calculation approaches the pulse period the sub vectors become more predictable as they sample the rising and falling edges of the pulse, resulting in a decrease in entropy for values of τ close to, but not equal to the pulse period. These are the dips seen either side of the peaks in Figs. 2(b) and 3(b).

At the point where the ordinal pattern delay matches the pulse period, if the pulse amplitudes are not exactly equal then the entropy will spike to a higher value which approximately quantifies the complexity of the pulse peak amplitude variation. This "inverted dip" feature is found to be typical of dynamics with regularly occurring spikes with different amplitudes. This feature is more prominent in the case of the OISSL data, seen in Fig. 3(b), due to the pulse shape being more regular than in the VCSEL case in Fig. 2.

To explore the dependence of PE/WPE analysis on amplitude and temporal variation of pulse-like time series in a more systematic way appropriate simulations are carried out in the following section.

4. Simulating random amplitude and temporal variations to pulses

Simulated time series of pulsed signals were generated to check the behavior of the WPE analysis with varying levels of amplitude and temporal noise. A clean signal was generated using a high order sine function $y = \sin^{20}(x)$ with 20,096 points sampled at $\Delta x = \pi/158$. The time series contains 128 pulse events with a period of π or 158 sampling points. For this clean signal, where each pulse has exactly the same amplitude, the permutation entropy drops to zero when the ordinal pattern delay τ exactly matches the pulse period (π). In this situation all values of the sub vector are equal and therefore the probability distribution has only one element with a value of 1, with the remaining $D!$ possible ordinal patterns having a probability of zero. To investigate the effect of unequal pulse amplitudes, each pulse was multiplied by a very small random number (between 1 and 10^{-5} and $1 + 10^{-5}$). The plot comparing the WPE calculated from the clean and perturbed signals is shown in Fig. 4(b). The sharp peak at τ = 158 (pulse period) observed for the perturbed signal is similar to that observed in the pulsed laser systems in Fig. 2 and Fig. 3. This provides a first indication that the WPE peak can be caused by inequalities in the pulse amplitudes.

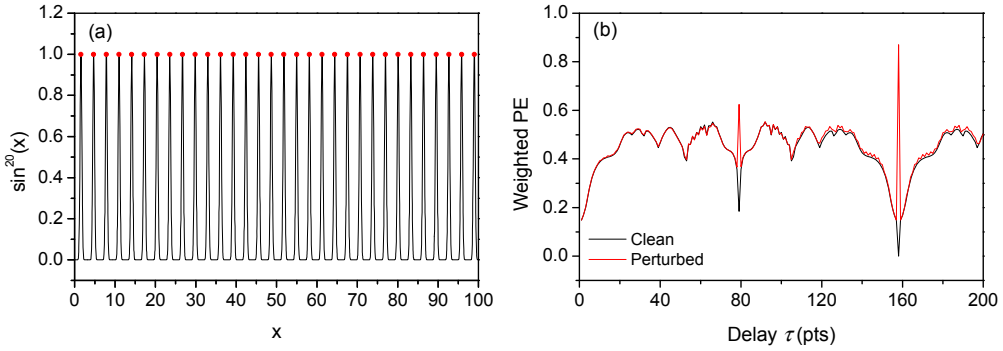

Fig. 4. (a) Simulated clean pulsed time series $y = \sin^{20}(x)$. (b) Weighted PE (D = 5) as a function of ordinal pattern delay for a time series of clean simulated pulses (black trace) and the clean signal with each pulse multiplied by a small random number between 1 ± 10^{-5} (red trace).

4.1 Amplitude noise

To investigate the effect of pulse amplitude variation in a more systematic way, simulated amplitude noise was added to the signal by multiplying each pulse in the clean time series by a random number with uniform distribution between 1–AN and 1 + AN, where AN is the "amplitude noise level" (e.g. when AN = 0.08, each pulse has a random amplitude between

#208715 - $15.00 USD Received 24 Mar 2014; revised 5 May 2014; accepted 4 Jul 2014; published 16 Jul 2014

0.92 and 1.08). The permutation analysis as a function of ordinal pattern delay is shown in Fig. 5 for values of AN = 0.01, 0.02, …, 0.09, 0.1. Note that these WPE plots represent discrete delay values so the continuous curves are only displayed for visual clarity.

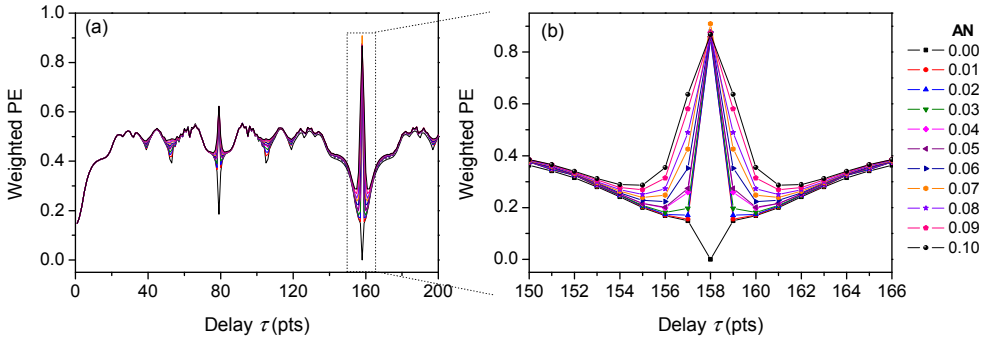

Fig. 5. (a) Weighted PE ($D = 5$) as a function of ordinal pattern delay for simulated pulses with added amplitude noise. (b) Magnified section around delay $\tau = 158$ (pulse period).

The results, presented in Fig. 5, confirm the observations made before in Fig. 4. The amplitude noise induces a peak within a broader valley in the WPE at the pulse period. The depth of the valley either side of the peak decreases with increasing noise level. The width of the peak also increases slightly but due to the discrete nature of the plot and relatively narrow width (only several points), it is not a very sensitive measure of the amplitude noise level.

For increased levels of noise, the depth of the valley, measured as the minimum value of WPE reached either side of the peak at $\tau = 158$, increases linearly as seen in Fig. 6(a). This is observed as a result of the time series points adjacent to the pulse peak becoming larger than the peak of neighboring pulses.

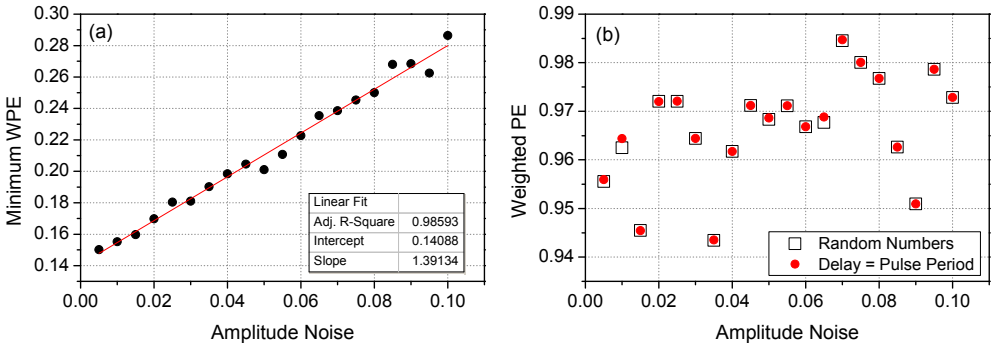

Fig. 6. (a) Minimum value of WPE either side of the peak at $\tau = 158$ and linear fit. (b) Weighted permutation entropy ($D = 4$) for the random numbers used to generate pulse amplitude noise with $\tau = 1$, and WPE of the pulses with $\tau = 158$. Ordinal pattern length $D = 4$ was used to satisfy the requirement that $N \gg D!$.

The level of amplitude noise has little effect on the maximum value of the weighted permutation entropy at $\tau = 158$. This invariance of the maximum WPE value to amplitude noise is expected since it is only based on the relative order of the points. The value of the WPE at the peak is mostly indicative of the complexity of the set of random numbers used to generate the pulse amplitudes for that particular noise level. This is illustrated by the plot in Fig. 6(b) which shows the WPE calculated on the random numbers used to generate the simulated pulse amplitudes with delay $\tau = 1$ ($D = 4$) and the WPE of the time series with delay $\tau = 158$ ($D = 4$). Since the number of points being analyzed here is $N = 128$ (i.e. the number of pulses), an ordinal pattern length of $D = 4$ was used in this case in order to satisfy

#208715 - $15.00 USD Received 24 Mar 2014; revised 5 May 2014; accepted 4 Jul 2014; published 16 Jul 2014

the requirement that $N \gg D!$ [21]. For nearly all levels of noise the maximum WPE at delay $\tau = 158$ (red dots) is the same as the WPE calculated on the set of random numbers used for pulse amplitudes (black squares).

4.2 Temporal noise

Temporal noise in the form of pulse timing jitter was simulated by shifting each pulse in the clean signal so that the pulse interval was a random integer number of points between 158 ± TN point, where TN is the "temporal noise level" (e.g. when TN = 8 the period between each pulse is a random integer number between 150 and 166 points). The permutation analysis as a function of ordinal pattern delay is shown in Fig. 7 for values of TN = 1, 2, …, 9, 10. There was no amplitude noise included in these simulations.

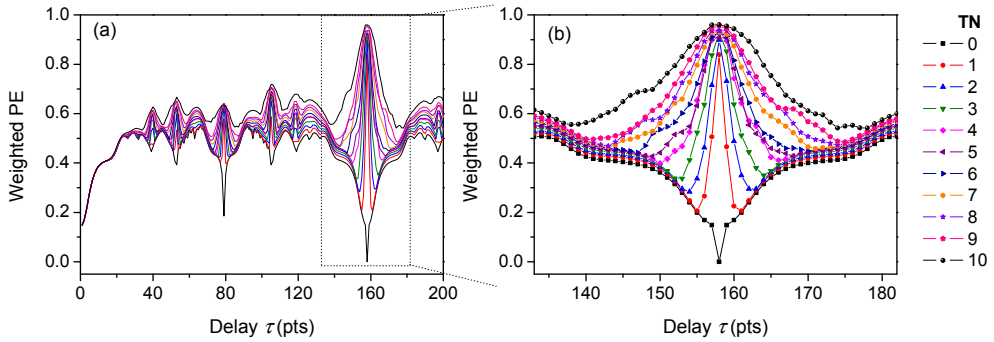

Fig. 7. (a) Weighted PE ($D = 5$) as a function of ordinal pattern delay for simulated pulses with added temporal noise. (b) Magnified section around delay $\tau = 158$.

The plots in Fig. 7 demonstrate that timing jitter also induces a peak in the WPE within the broader valley around the pulse period at $\tau = 158$. Increased timing jitter causes the peak to broaden and appears to have a much greater impact on the width than amplitude noise.

A measurement of the WPE at local minima, as done for the amplitude noise analysis in Fig. 6(a), was not possible for these temporal noise simulations due to the WPE being asymmetric and deformed, especially at larger levels of timing jitter. Instead, the width of these peaks was measured as the number of points between the local minima either side of the peak. This width can be seen to increase systematically with increasing temporal noise level in Fig. 8.

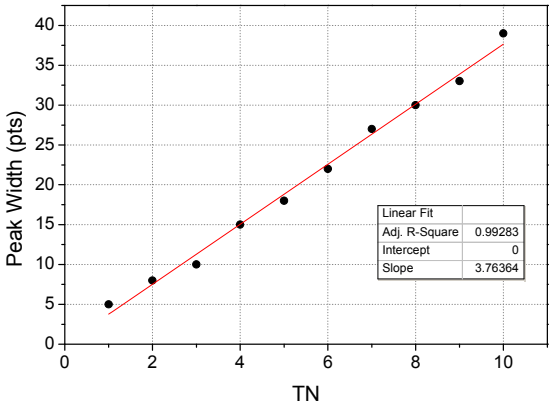

Fig. 8. Width of the WPE peak around $\tau = 158$ for simulated pulses with added temporal noise and least-square fit to a straight line.

#208715 - $15.00 USD Received 24 Mar 2014; revised 5 May 2014; accepted 4 Jul 2014; published 16 Jul 2014

Clearly the pulse timing jitter has a more significant effect on the width of the WPE peak. In the simulations used here the maximum amplitude noise signal (AN = 0.1) measured a 5.88% standard deviation of the mean amplitude, which produced a WPE peak width (measured as the number of points between the local minima) of 5 points. For the timing jitter simulations, the maximum temporal noise level (TN = 10) produced a time series with 5.71% standard deviation from the mean pulse period and resulted in a WPE peak width of 39 points. There does not appear to be a simple way to distinguish the effects of amplitude noise and timing jitter from the WPE plots alone.

5. Discussion

These simulations are able to provide some insights into the experimental results for the VCSEL and OISSL systems. Comparison between the WPE plots for the VCSEL data in Fig. 2(b) and OISSL data in Fig. 3(b) reveals the minimum value of WPE either side of the central peak was lower for the OISSL data and the peak width was also narrower, indicating lower levels of amplitude noise and timing jitter in the OISSL time series. Statistics on the peaks in each time series shows the VCSEL data as having pulse periods with 7.5% standard deviation about the mean, and 22.0% standard deviation in amplitude, compared with a timing jitter of 1.3% and amplitude variation of 2.5% in the OISSL time series.

#208715 - $15.00 USD Received 24 Mar 2014; revised 5 May 2014; accepted 4 Jul 2014; published 16 Jul 2014

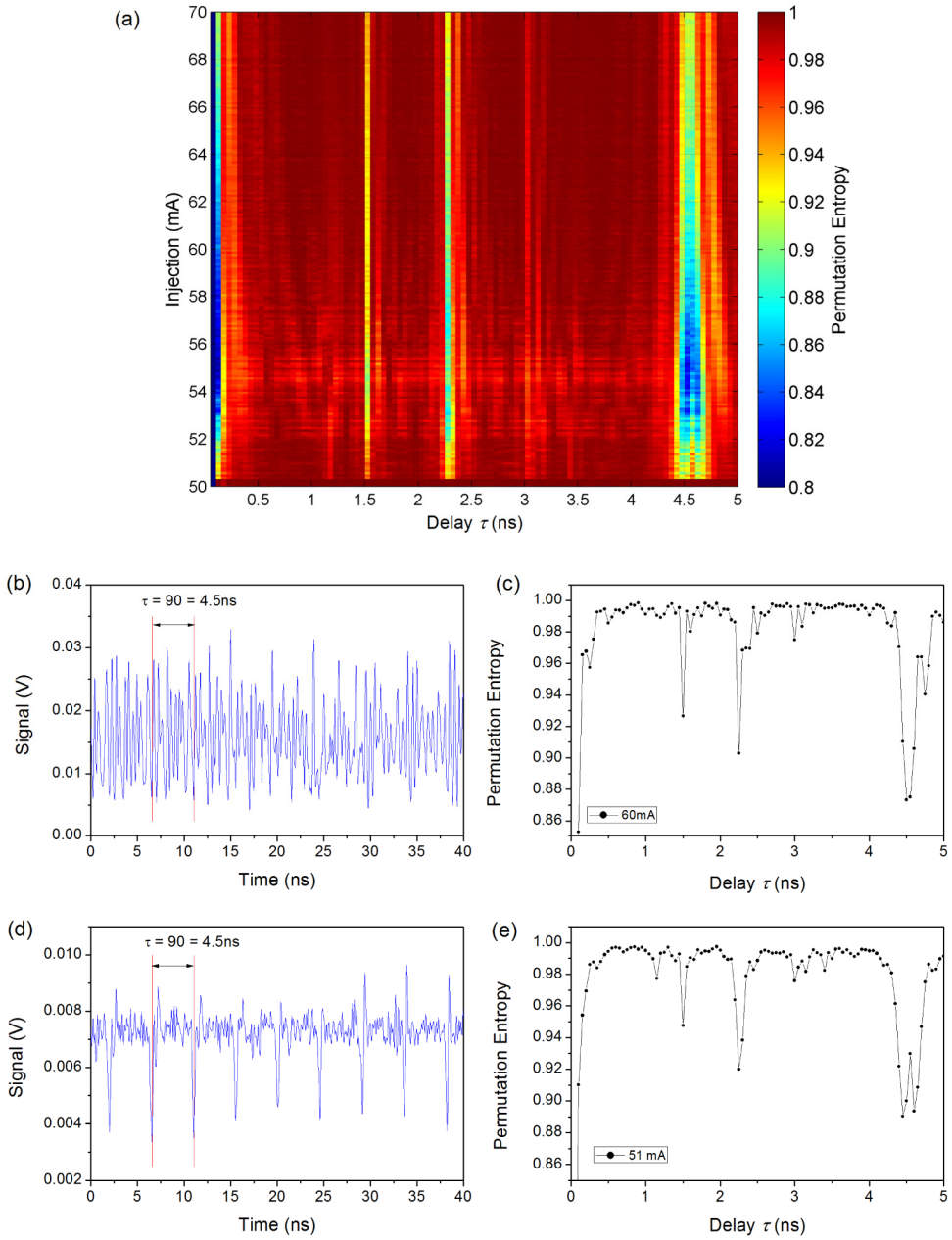

Fig. 9. (a) Map of PE as a function of ordinal pattern delay and injection current from a semiconductor laser with optical feedback (reproduced from [10]). Two examples of measured time series and PE as a function of τ from regions of the map where no inversion is observed at 60 mA (b)-(c) and where inversion occurs due to pulsed operation (d)-(e).

Permutation entropy analysis is proving to be a very useful technique for quantifying complexity and is becoming a standard tool employed by those working in nonlinear time series analysis. Routine application of this technique could assist in identifying if a data set has a pulsed component by looking for the 'inverted dip' behavior in plots of PE/WPE as a function of ordinal pattern delay. The presence of such a signal can prompt further

#208715 - $15.00 USD Received 24 Mar 2014; revised 5 May 2014; accepted 4 Jul 2014; published 16 Jul 2014

investigation into the cause of the periodicity, and in turn provides insight into the nonlinearity and laser physics of the system.

This interpretation of PE/WPE plots provides an explanation for a previously unexplained feature observed in maps of the PE as a function of ordinal pattern delay for a semiconductor laser with conventional optical feedback [10]. In this previous work, an apparent splitting of the dip associated with the external cavity round trip time was observed at low injection currents, as seen in Fig. 9(a). At the time there was no clear explanation for the cause of this observation. In the light of the work report here, this splitting can now be understood as a broadening of the dip and an inversion of the central part resulting from the transition to a fairly regular pulsed operation of the laser. The nature of the time series corresponding to two regions of the map can be seen in Figs. 9(b) and 9(c), where the dip occurs at the external cavity delay with no inversion, and in Figs. 9(d) and 9(e), where the inversion occurs.

The plot in Fig. 9(c) shows the PE dipping at the external cavity round trip time (τ = 4.5 ns) and Fig. 9(a) the time series from which it was calculated shows fully developed chaotic operation at 60 mA. At an injection current of 51 mA the PE plot in Fig. 9(e) show the inverted peak resulting from the pulsed laser operation shown in Fig. 9(e).

This example illustrates the usefulness of this technique to identify regions of pulsed dynamics which may have otherwise been missed.

6. Comparing stochastic simulations with nonlinear laser dynamics

In the simulated pulsed signals the amplitude and temporal variations are generated from a pseudo-random process and therefore should have maximum entropy i.e. very close to 1. It is unknown whether the source of the variation in the experimental laser signals is stochastic or deterministic, or a mixture of both. To investigate this, WPE analysis has been performed on just the values of the experimental time series pulse peaks and inter-pulse periods (similar to the approach used in [11–13]) for both the optically injected solid state laser (OISSL) [14] and vertical cavity surface emitting laser (VCSEL) with frequency selective optical feedback [19, 20] to see if any deterministic structure exists. A peak detection algorithm identified all the pulses in the experimental time series, shown as red dots in Figs. 2 to 4. The amplitude and interval between each were recorded and analyzed using PE and WPE with ordinal pattern length D = 4 and ordinal pattern delay τ = 1. Since we are only using the pulse amplitudes and pulse intervals, rather than the full time series, we have much lower N (see second column in Table 1). As such we use D = 4 so that $N \gg D!$ is satisfied. The results are summarized in Table 1.

Table 1. PE and weighted PE for the pulse amplitudes and pulse intervals of the experimental time series.[a]

Laser system	No. of pulses	Pulse Amplitude WPE	Pulse Amplitude PE	Pulse Period WPE	Pulse Period PE
OISSL	200	0.8653	0.9012	0.7134	0.3581
VCSEL	1634	0.9719	0.9895	0.9378	0.9516
VCSEL	200 (x8 sections)	0.9408 (mean) 0.0406 (st. dev.)	0.9396 (mean) 0.0194 (st. dev.)	0.9150 (mean) 0.0259 (st. dev.)	0.9376 (mean) 0.0164 (st. dev.)
SLWOF	2612	0.9959	0.9991	0.9334	0.9566

[a]The VCSEL data were analyzed as a whole (line 2) and in eight segments of 200 points (line 3). The variation of the results (characterized by the standard deviation) gives some indication of the absolute accuracy of the PE numbers.

The semiconductor laser with optical feedback (SLWOF) system [10] is included even though it is not a pulsed signal just for comparison with a highly complex system. The time series are the same as those described in Section 3.

These results suggest that the solid state laser system (OISSL) produces pulsed dynamics which are more predictable than the semiconductor laser systems (VCSEL and SLWOF). In particular, the non-uniform probability distribution of the sequence of intervals between

#208715 - $15.00 USD Received 24 Mar 2014; revised 5 May 2014; accepted 4 Jul 2014; published 16 Jul 2014

consecutive pulses in the OISSL system indicates that certain patterns are more likely to occur than others. The value of PE for the OISSL pulse period is significantly less than the WPE value. This is due to the very regular pulsing of the OISSL system resulting in the ordinal patterns of inter-pulse period having a lot of equal values. In calculating standard PE, these patterns contribute equally to the probability distribution giving a large count value for that particular pattern. The application of the variance weighting, given in Eq. (5), to these ordinal patterns when calculating WPE means the patterns with equal values (zero variance) do not contribute to the pattern counts.

The number of pulses in the OISSL system was restricted to 200 due to experimental limitations. To ensure the lower entropy values were not due to fewer samples, the PE/WPE analysis on the VCSEL data was also limited to 200 pulse samples. Analysis was performed on 8 sections of 200 pulses in the VCSEL data and the results showed the mean entropy was always lower than the value calculated for the complete 1634 pulses in the VCSEL data set. However, this mean value was still significantly higher than the value calculated for the OISSL system.

This result supports previous work which shows the solid state system is less complex than semiconductor laser dynamics [18, 23]. In these studies, the correlation dimension [1] was employed in an attempt to characterize the complexity of experimental systems. The technique could be successfully applied to the OISSL system in most regions of the parameter space [18], but was unable to characterize any of the time series from the non-periodic regions of operation for the more complex SLWOF system [23]. The PE/WPE values obtained for the VCSEL and SLWOF systems are consistent with those obtained for the random variation simulated data. Thus, the PE/WPE values do not support that the pulse timing or amplitude variations are deterministic in these cases.

7. Conclusion

The permutation entropy (PE) and weighted PE provide a relative measure of complexity based on ordinal patterns present in time series data. Previous work has shown that when applied to output power time series measured from nonlinear laser systems, PE/WPE as a function of ordinal pattern delay decreases at delay times corresponding to key frequencies associated with the laser systems [9, 10], in effect indicating that the dynamics become more predictable on those time scales. Application of this technique on spiky, pulsed time series data from experimental laser systems revealed a similar drop in WPE for values of delay surrounding dominant pulse period, but resulted in an unexpected inversion of the central part of this dip where the delay exactly matched to the pulse period. The reason for this is that the permutation vectors, constructed with values of τ just below and just above the pulse period, sample the rising and falling edges of the pulses and are represented by the same ordinal patterns. This increased occurrence of certain patterns results in a drop in the permutation entropy at these delays. When the values of τ matches the pulse period then the WPE will either drop to zero, if the pulse amplitudes are equal, or will increase to a value which quantifies the entropy of the probability distribution of the pulse amplitudes. In the case where the pulses have randomly varying amplitude the WPE will approach 1. This feature was observed in WPE plots for output power time series recorded from a vertical cavity surface emitting laser with frequency selective feedback [16] and an optically injected solid state laser [14].

Simulations of pulsed time series with varying levels of amplitude and temporal noise revealed the minimum value of WPE on either side of the central peak and also the width of the inverted WPE peak can be used as a relative measure of the level of noise in pulse amplitude and/or pulse period. It was found that timing jitter affects these measures more than amplitude jitter. The ‘inverted-dip-peak’, present in the plot of PE/WPE as a function of ordinal pattern delay τ, emerges as a signal to identify pulsed dynamics (albeit with some

#208715 - $15.00 USD Received 24 Mar 2014; revised 5 May 2014; accepted 4 Jul 2014; published 16 Jul 2014

level of amplitude and/or temporal noise) in nonlinear laser systems where otherwise this might have been missed if researchers are not studying the detail of the time series data.

Applying the PE analysis directly to the amplitude of the pulses and/or the timing between pulses can indicate whether there are any patterns that are more probable than others. The results reported here suggest that the pulses produced by an optically injected solid state laser (operated in a reasonably stable parameter space) have amplitude and temporal characteristics which are more predictable than the semiconductor laser based feedback systems studied.

Overall, this research shows how PE and WPE are good tools for identifying complex and pulsed outputs. This can assist to show where transitions from complex nonlinear outputs to more standard outputs such as mode-locked pulsed sequences may be being frustrated from occurring, or could occur with some additional control in the system.

Acknowledgments

This research was supported in part by the Australian Research Council (Linkage Project LP100100312), Sirca Technology Pty Ltd, Macquarie University, the Science and Industry Endowment Fund (RP 04-174). Also, funding from the Royal Society (London) for the cooperation between the groups is gratefully acknowledged. The raw data for the VCSEL system, shown in Fig. 2, were obtained by Neal Radwell during his thesis work [20]. The raw data for the OISSL system, shown in Fig. 3, were generated by Simo Valling, Thomas Fordell and Asa Lindberg in the Department of Physics, University of Helsinki. We are grateful to Dr Radwell and Dr Lindberg and her group for sharing their experimental results with us.

#208715 - $15.00 USD Received 24 Mar 2014; revised 5 May 2014; accepted 4 Jul 2014; published 16 Jul 2014